Controller Tuning by means of Multi-objective Optimization Algorithms: a Global Tuning Framework

Gilberto Reynoso-Meza, Sergio García-Nieto, Javier Sanchis, and Xavier Blasco

Abstract

A holistic multi-objective optimization design technique for controller tuning is presented. This approach gives control engineers greater flexibility to select a controller that matches their specifications. Furthermore, for a given controller it is simple to analyse the trade-off achieved between conflicting objectives. By using the multi-objective design technique it is also possible to perform a global comparison between different control strategies in a simple and robust way. This approach thereby enables an analysis to be made of whether a preference for a certain control technique is justified. This proposal is evaluated and validated in a non-linear MIMO system using two control strategies: a classical PID control scheme and a feedback state controller.

Index Terms

multiobjective optimization, controller tuning, pid tuning, evolutionary algorithm, decision making.

Acronyms

DM	Decision maker
EA	Evolutionary algorithm
GPP	Global physical programming
IADU	Integral of the absolute value of the derivative control signal

Instituto Universitario de Automática e Informática Industrial, Universitat Politècnica de València, Camino de Vera s/n , Valencia 46022, Spain (email: gilreyme@posgrado.upv.es; http://ctl-predictivo.upv.es)

IAE	Integral of the absolute value of the error
ISA	Instrumentation, systems and automation society
LD	Level diagram
MIMO	Multiple-input multiple-output
MOEA	Multi-objective evolutionary algorithm
mood4ct	Multi-objective optimisation design for controller tuning
MOO	Multi-objective optimisation
PI	Proportional-integral
PID	Proportional-integral-derivative
SISO	Single-input single-output
SS	State space
TITO	Two-input two-output
TRMS	Twin rotor MIMO system

I. Introduction

Satisfying a set of specifications and constraints required by real-control engineering problems is often difficult with traditional optimization approaches. From the control point of view it is common to face a variety of requirements and specifications. These range from time-domain specifications (such as maximum overshoot, settling time, steady state error, raise time) to frequency-domain requirements (noise rejection or multiplicative uncertainty, for example). Furthermore, constraints such as saturations, or the maximum changes enabled for a control signal may be considered. Such problems, when multiple objectives must be fulfilled, are known as multi-objective problems.

A traditional approach for solving a multi-objective problem is to translate it into a single-objective problem using weighting factors to indicate the relative importance among objectives (see for example [1]). The solution obtained strongly depends on which factors are used, and it is not usually a trivial task to select the right weighting vector to assure a quality solution with a reasonable trade-off among objectives [2]. This situation may be more complicated when constraints are considered. More complex methods to tackle these issues have been developed [3], such as lexicographic methods, goal programming methods or physical programming [4].

Multi-objective optimization (MOO) can handle these issues in a simple manner because of its simultaneous optimization approach. In MOO, all the objectives and constraints are significant from the designer point of view, and as a consequence, each is optimized to obtain a set of optimal non-dominated solutions. The MOO approach offers to the designer a set of solutions, a Pareto set approximation, where all the solutions are Pareto-optimal [3]. This set of solutions offers the decision maker (DM) greater flexibility. The role of the designer is to select the most preferable solution according to her/his needs and preferences for a particular situation.

There are several widely used algorithms for calculating this Pareto set approximation (normal boundary intersection method [5], normal constraint method [6], and successive Pareto front optimization [7]). Recently, multi-objective evolutionary algorithms (MOEAs) have started to be used because of their flexibility in dealing with non-convex and highly constrained functions [8], [9]. Some examples include NSGA-II [10], MOGA [11], ev-MOGA [12], paϵ-MyDE [13], and sp-MODE [14]. General methodologies for MOO have been developed [15]; nevertheless new approaches and methodologies using MOO are still required focusing on controller tuning.

In this work, a holistic MOO design technique using MOEA's is presented for controller tuning purposes. In Section II a review on MOO is given and in Section III the MOO approach for controller tuning (*mood4ct*) is presented. In Section IV an engineering application example is developed and experimentally evaluated and discussed. Finally, some concluding remarks and future work are given.

II. Multi-objective optimization review

A MOO problem, without loss of generality, [1] can be stated as follows:

$$\min_{\boldsymbol{\theta} \in \Re^n} \boldsymbol{J}(\boldsymbol{\theta}) \quad = \quad [J_1(\boldsymbol{\theta}), \ldots, J_m(\boldsymbol{\theta})] \in \Re^m \tag{1}$$

where $\boldsymbol{\theta} \in \Re^n$ is defined as the decision vector, and $\boldsymbol{J}$ as the objective vector. In general, there is no single solution because there is no solution that is better than the others for all the objectives. Therefore, a set of solutions, the Pareto set $\boldsymbol{\Theta_P}$, is defined and its projection into the

[1] A maximization problem can be converted to a minimization problem. For each of the objectives that have to be maximized, the transformation $\arg\max_{\boldsymbol{\theta}} J_i(\boldsymbol{\theta}) = \arg\min_{\boldsymbol{\theta}}(-J_i(\boldsymbol{\theta}))$ can be applied.

objective space is known as the Pareto front $\boldsymbol{J_P}$ (see Figure 1). Each point in the Pareto front is said to be a non-dominated solution (see Figure 2). A given solution $\boldsymbol{\theta}^{\mathbf{1}}$ dominates a second solution $\boldsymbol{\theta}^{\mathbf{2}}$ only if $\boldsymbol{\theta}^{\mathbf{1}}$ has a better or equal cost value for all objectives (with, at least, one cost value being better).

Definition (Dominance relation): given a solution $\boldsymbol{\theta}^{\mathbf{1}}$ with cost function value $\boldsymbol{J}(\boldsymbol{\theta}^{\mathbf{1}})$, it dominates a second solution $\boldsymbol{\theta}^{\mathbf{2}}$ with cost value $\boldsymbol{J}(\boldsymbol{\theta}^{\mathbf{2}})$ if and only if:

$$\{\forall i \in [1, 2, \ldots m], J_i(\boldsymbol{\theta}^{\mathbf{1}}) \leq J_i(\boldsymbol{\theta}^{\mathbf{2}})\}$$
$$\wedge$$
$$\{\exists q \in [1, 2, \ldots m] : J_q(\boldsymbol{\theta}^{\mathbf{1}}) < J_q(\boldsymbol{\theta}^{\mathbf{2}})\}$$

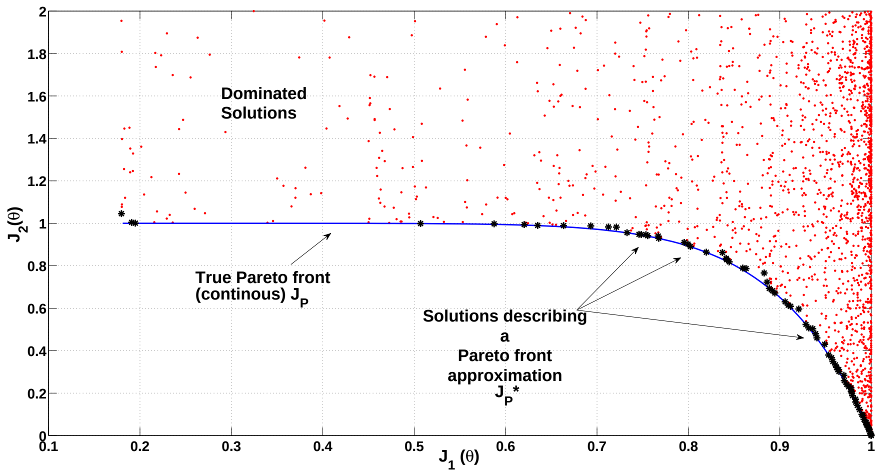

Fig. 1: Pareto front concept (example of a two objective optimization problem).

MOO techniques search for a discrete approximation $\Theta_{\boldsymbol{P}}^*$ of the Pareto set $\Theta_{\boldsymbol{P}}$ with a good description $\boldsymbol{J_P^*}$ of the Pareto front. In this way, the DM has a set of solutions for a given problem and more flexibility for choosing a particular or desired solution.

III. Multi-objective optimization design approach for controller tuning

As a global framework, three main objectives need to be considered in a controller's tuning procedure: performance, robustness and implementation issues. Usually, classical controller tuning techniques have been developed for only one of those objectives. Other tuning techniques are able

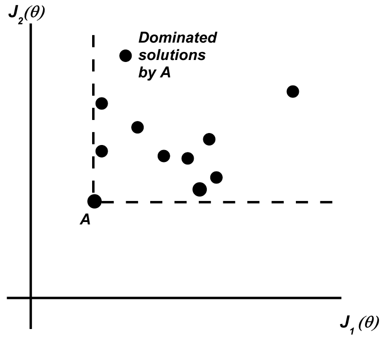

Fig. 2: Dominance concept. Solution A has a better cost value for all objectives.

to deal with these objectives. For example, H_2/H_∞ designs (or mixed-sensitivity techniques) have been shown to be powerful tools to address the trade-off between performance and robustness. However it is not easy to include constraints in the control and/or process variables and the performance objective interpretability could be lost. Strategies as Model Predictive Control [16] deal with this problem solving an optimization statement in each sampling time. A quadratic measure is usually used, whereas an absolute error measurement could be helpful to the designer for interpreting the performance of a proposed controller. However, useful or interpretable objectives considered by the DM could lead to complex non-convex and highly constrained cost functions.

Evolutionary algorithms (EAs) are a flexible tool for handling non-convex cost functions that are highly constrained in decision and objective spaces. They have been successfully applied in several control engineering areas [17] such as controller tuning [18], PI-PID tuning [19]–[21], multivariable control [22]–[26], and fuzzy control [27]–[30]. These algorithms have also been merged together with predictive control [31], H_∞ techniques [32], [33], linear matrix inequalities [34], and loop shaping [35]. The use of such a class of algorithms leads to a higher degree of flexibility, since more interpretable objectives can also be used to tune any kind of controller. Therefore, a multi-objective optimization design for controller tuning (*mood4ct*) by means of evolutionary algorithms will be proposed. Any multi-objective optimisation design approach must follows three main steps: problem definition, multi-objective optimisation process and decision making stage (see figure 3). The main contribution of this work consists in define a global optimisation problem statement for multivariable processes and its integration into the optimisation procedure and the decision making stage (which is not a trivial task when the number of objectives is three or more). Any kind of MOEA can be used (NSGA-II [10] [2], MOGA [15], [36][3], ev-MOGA [12][4], paϵ-MyDE [13], and sp-MODE [14], among others). Such algorithm must be capable of converging towards the Pareto front; it must have a good constraint handling mechanism and it must compute a useful well-spread approximation along the Pareto front.

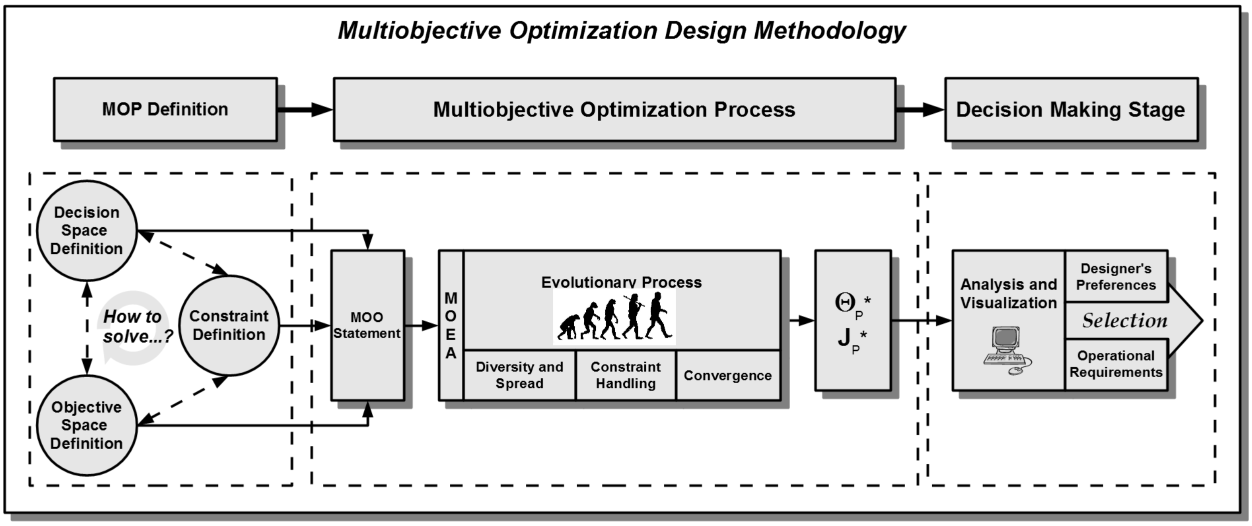

Fig. 3: Multi-objective optimisation design methodology.

The *mood4ct* approach, roughly speaking, is based on:

- A highly reliable process model to obtain a measurement of the performance for a given controller.
- Meaningful process objectives to facilitate the decision making stage.
- A MOEA with a constraint handling mechanism which can assure convergence, spread and diversity into the Pareto front.
- An intuitive and easy-to-use tool to analyze m-dimensional Pareto fronts.

[2]Source code available at: http://www.iitk.ac.in/kangal/codes.shtml; also, a variant of this algorithm is available in the global optimization toolbox of Matlab.

[3]Genetic Algorithm toolbox for Matlab available at http://www.sheffield.ac.uk/acse/research/ecrg/gat

[4]Available for Matlab at: http://www.mathworks.com/matlabcentral/fileexchange/31080

A. Process objectives

The use of a process model will lead to a higher degree of reliability for the controller's performance under practical considerations such as saturation, complex tracking references, and/or any kind of constraint. In this work, the integral of the absolute magnitude of the error (IAE) and the integral of the absolute value of the derivative control signal (IADU) are used due to their interpretability. Given a model, which will be controlled with a sampling time of T_s with $t \in [t_0, t_f]$ and with controller tuning parameters $\boldsymbol{\theta}$, the IAE and IADU are defined as:

$$IAE(\boldsymbol{\theta}) = T_s \sum_{k=1}^{N} |r_k - y_k| \tag{2}$$

$$IADU(\boldsymbol{\theta}) = \sum_{k=1}^{N} |u_k - u_{k-1}| \tag{3}$$

Where r_k, y_k and u_k are respectively the setpoint signal, the controlled and manipulated variables at sample k; while N is the number of samples in $[t_0, t_f]$. The above mentioned objectives are defined for a SISO system. If a MIMO system with ρ inputs and ν outputs is under consideration, it is possible to have as many objectives IAE, $IADU$ as inputs and outputs. Nevertheless, this could lead to an exponential increase in the number of solutions in the Pareto front $\boldsymbol{J}_P^*$, and the analysis on the results could be more difficult. Moreover, a large subset of solutions will probably be undesirable for the DM (for example, controllers with an outstanding performance in one controlled variable at the expense of another). So, it is worthwhile trying to reduce the objective space to facilitate the analysis for the DM without losing any of the advantages of the MOO approach [37]. Let it be:

$$\boldsymbol{J}_E(\boldsymbol{\theta}) = \left[\frac{IAE^{1,1}(\boldsymbol{\theta})}{\Delta R^1}, \frac{IAE^{2,2}(\boldsymbol{\theta})}{\Delta R^2}, \ldots, \frac{IAE^{\nu,\nu}(\boldsymbol{\theta})}{\Delta R^\nu} \right] \tag{4}$$

$$\boldsymbol{J}_U(\boldsymbol{\theta}) = \left[\sum_{j=1}^{\nu} \frac{IADU^{1,j}(\boldsymbol{\theta})}{\Delta U^1_{max}}, \sum_{j=1}^{\nu} \frac{IADU^{2,j}(\boldsymbol{\theta})}{\Delta U^2_{max}}, \ldots, \sum_{j=1}^{\nu} \frac{IADU^{\rho,j}(\boldsymbol{\theta})}{\Delta U^\rho_{max}} \right] \tag{5}$$

Where $IAE^{i,j}(\boldsymbol{\theta})$ is the $IAE(\boldsymbol{\theta})$ for controlled variable i when there is a setpoint change ΔR^j for controlled variable j; $IADU^{i,j}(\boldsymbol{\theta})$ is the $IADU(\boldsymbol{\theta})$ for control signal i when there is a change in setpoint signal j, and ΔU^i_{max} is the maximum change allowed for control signal i. Vectors 4 and 5 contain the IAE and IADU values for each variable normalized over a work range. Because of this, it is possible to perform a comparison between controlled variables and between control signals.

Define a sorting function $\mathcal{Z} : \Re^{1\times n} \rightarrow \Re^{1\times n}$, $\mathcal{Z}(\boldsymbol{f}) = \boldsymbol{g}$ so that: $\boldsymbol{g} = [a_1, a_2, a_3, \ldots, a_n]$, where $a_1 \geq a_2 \geq a_3 \geq \ldots a_n$, where each a_i is an element of $\boldsymbol{f}$. The global index for IAE and IADU performance measurements are defined as $J_{\mathcal{E}}(\boldsymbol{\theta})$ and $J_{\mathcal{U}}(\boldsymbol{\theta})$ respectively:

$$J_{\mathcal{E}}(\boldsymbol{\theta}) = \mathcal{Z}(\boldsymbol{J}_E(\boldsymbol{\theta})) \times \boldsymbol{w} \tag{6}$$

$$J_{\mathcal{U}}(\boldsymbol{\theta}) = \mathcal{Z}(\boldsymbol{J}_U(\boldsymbol{\theta})) \times \boldsymbol{w} \tag{7}$$

Vector $\boldsymbol{w}$ indicates it is most important to optimize the maximum value, thereby assuring a minimum worst performance for all objectives. As inputs and outputs are usually normalized in the range $[0, 1]$ an intuitive value [5] for $\boldsymbol{w}$ is $\boldsymbol{w} = [10^0, 10^{-2}, \ldots, 10^{-n}]^T$.

Please note that this objective reduction is important to facilitate the decision making step. In one hand, the multi-objective approach gives to the DM a better insight concerning the objective trade-offs; in the other hand, too much information (too many objectives) can hinder the DM task to select a desired solution. This topic, known as many-objectives optimization (usually more than 4 objectives) is not trivial, and some algorithms could face several problems due to their diversity improvement mechanisms [38], [39]. The objective reduction is an alternative to face the many-objectives optimization issue [40], and with this proposal the relevant information about the conflict between control actions and performance is retained.

Additionally, a measurement for coupling effects is required:

$$\boldsymbol{J}_C(\boldsymbol{\theta}) = \left[\max_{i\neq 1} \frac{IAE^{1,i}(\boldsymbol{\theta})}{\Delta R^i_{max}}, \max_{i\neq 2} \frac{IAE^{2,i}(\boldsymbol{\theta})}{\Delta R^i_{max}}, \ldots, \max_{i\neq \nu} \frac{IAE^{\nu,i}(\boldsymbol{\theta})}{\Delta R^i_{max}} \right], i \in [1, 2, \ldots, \nu] \tag{8}$$

$$J_{\mathcal{C}}(\boldsymbol{\theta}) = \mathcal{Z}(\boldsymbol{J}_C(\boldsymbol{\theta})) \times \boldsymbol{w} \tag{9}$$

Where ΔR^i_{max} is the maximum allowable setpoint step change for controlled variable i.

[5] Notice that setting $w = [1, 0, \ldots, 0]$ is equivalent to set $J_{\mathcal{E}}(\boldsymbol{\theta}) = \|\boldsymbol{J}_E(\boldsymbol{\theta})\|_\infty$. Nevertheless, any MOEA would not be able to differentiate, for example, between one solution $\boldsymbol{J}_E(\boldsymbol{\theta}^1) = [0.9, 0.9, 0.9, 0.9, 0.9]$ with $\mathcal{Z}(\boldsymbol{J}_E(\boldsymbol{\theta}^1)) \times \boldsymbol{w} = 0.9$ from another one $\boldsymbol{J}_E(\boldsymbol{\theta}^2) = [0.9, 0.5, 0.01, 0.5, 0.7]$ with $\mathcal{Z}(\boldsymbol{J}_E(\boldsymbol{\theta}^2)) \times \boldsymbol{w} = 0.9$. The latter should be preferred over the former.

Finally, it is not possible to rely only on the process model, due to un-modeled dynamics or parametric uncertainty. Therefore, a robustness objective is required to guarantee a robust stability. One possible choice is to use complementary sensitivity function $\mathcal{T}(s)$ with a linearized process model as follows:

$$J_{\mathcal{T}} \quad = \quad \sup_{\omega} \bar{\sigma}\left(\mathcal{T}(\jmath\omega)W(\jmath\omega)\right), \omega \in (\overline{\omega}, \underline{\omega}) \tag{10}$$

Usually $\mathcal{T}(s)$ together with weighting function $W(s)$ is stated as a hard constraint ($J_{\mathcal{T}} < 1$). Since $W(s)$ selection is not a trivial task [41], the *mood4ct* approach can manage this task as an optimization objective (*i.e.*, it will be minimized instead of being used as a hard constraint). The *mood4ct* can deal with constraints in the same way it deals with each objective and represents a feasible alternative to constraint-handling [42], [43]. This approach, combined with an adequate tool to analyze m-dimensional Pareto fronts, is useful to analyze the impact of relaxing, if possible, one or more constraints.

With the above mentioned objectives, it is possible to build a MOO statement to adjust any kind of parametric controller (see eq. 11). That is, given a control structure with numerical parameters to adjust, the latter MOO problem can be stated, using as performance measurement information from the simulation process. The objectives cover the most important requirements for a controller: performance, control effort, coupling effects and robustness. Although these performance measurements have been proposed as first approximation, some other measures can be used (or added) by the DM.

$$\min_{\boldsymbol{\theta}\in\Re^n} \boldsymbol{J}(\boldsymbol{\theta}) = \left[\ J_{\mathcal{E}}(\boldsymbol{\theta}), J_{\mathcal{U}}(\boldsymbol{\theta}), J_{\mathcal{C}}(\boldsymbol{\theta}), J_{\mathcal{I}}(\boldsymbol{\theta}), J_{\mathcal{T}}(\boldsymbol{\theta})\ \right] \in \Re^5 \tag{11}$$

Since the implementation objectives $J_{\mathcal{I}}$ are related with a particular controller, they will be considered according to each specific case. Constraint handling depends on the selected algorithm and its own mechanisms. In general, the guidelines stated in [44] can be used to incorporate them into the cost function evaluation or into the MOO statement as and additional objective [42], [43].

B. Multiobjective evolutionary algorithm

As it was noticed earlier, any kind of MOO algorithm can be used in the multi-objective optimisation design methodology. A MOEA is selected due to its flexibility to handle complex functions. The MOEA will adjust the parameters of a given controller to be used in the closed loop process simulation. Then it will use the performance calculated from the simulation process to evolve the population to the Pareto front. In particular, the sp-MODE algorithm is selected [14], due to its performance in academic benchmarks for MOO algorithms and its flexibility for control purposes. This algorithm is based on Differential Evolution technique, which is a real-coded evolutionary algorithm.

C. Pareto front visualization

It is widely accepted that visualization tools are valuable and provide decision makers with a meaningful method to analyze the Pareto front and take decisions [45]. For two-dimensional problems (and sometimes for three-dimensional) it is usually straightforward to make an accurate graphical analysis of the Pareto front, but the difficulty increases with the dimension of the problem. Tools as VIDEO [46] can plot a fourth dimension by using a color-coding in the a 3-dimensional plot. Nevertheless, it is usual to state more than four objectives in an MOO process. Common alternatives to tackle an analysis in higher dimension are: Scatter diagrams, Parallel coordinates [47] and Level Diagrams [48]. Scatter diagrams use a 2-dimensional graph for each pair of objectives whilst Parallel coordinates plot a m-dimensional objective vector in a two dimensional graphs. The former becomes difficult to analyze when visualizing several objectives (since at least $\frac{m(m-1)}{2}$ plots are required); the latter, is a very compact way, but it loses clarity with large sets of data.

Level diagram (LD) visualization [48] helps us to perform an analysis of the obtained Pareto front $\boldsymbol{J}_P^*$, which is not a trivial task when the number of objectives is larger than three. It has been used with success in control systems up to 15 objectives [49], safety systems analysis [50] and engineering design [51]. As pointed in [52], LD visualization is one of the most useful methods to visualize m-dimensional Pareto fronts. LD visualization is based on the classification of the approximation $\boldsymbol{J}_P^*$ obtained. Each objective $J_q(\boldsymbol{\theta})$ is normalized with respect to its minimum and maximum values. That is:

$$\hat{\boldsymbol{J}}_{\boldsymbol{q}}(\boldsymbol{\theta}) = \left[\hat{J}_1(\boldsymbol{\theta}), \hat{J}_2(\boldsymbol{\theta}), \ldots, \hat{J}_q(\boldsymbol{\theta})\right], q \in [1, \ldots, m]. \tag{12}$$

where

$$\hat{J}_q(\boldsymbol{\theta}) = \frac{J_q(\boldsymbol{\theta}) - J_q^{min}}{J_q^{max} - J_q^{min}}, q \in [1, \ldots, m]. \tag{13}$$

and

$$\boldsymbol{J}^{min} = \left[\min_{J(\boldsymbol{\theta}) \in J_P^*} J_1(\boldsymbol{\theta}), \ldots, \min_{J(\boldsymbol{\theta}) \in J_P^*} J_m(\boldsymbol{\theta})\right] \tag{14}$$

$$\boldsymbol{J}^{max} = \left[\max_{J(\boldsymbol{\theta}) \in J_P^*} J_1(\boldsymbol{\theta}), \ldots, \max_{J(\boldsymbol{\theta}) \in J_P^*} J_m(\boldsymbol{\theta})\right] \tag{15}$$

To each normalized objective vector $\hat{\boldsymbol{J}}(\boldsymbol{\theta})$ a p-norm $\|\boldsymbol{x}\|_p := \left(\sum_{q=1}^{m} |x_q|^p\right)^{1/p}$ is applied to evaluate the distance to an ideal solution $\boldsymbol{J}^{ideal} = \boldsymbol{J}^{min}$. Common norms are:

$$\|\hat{\boldsymbol{J}}(\boldsymbol{\theta})\|_1 = \sum_{q=1}^{m} \hat{J}_q(\boldsymbol{\theta}) \tag{16}$$

$$\|\hat{\boldsymbol{J}}(\boldsymbol{\theta})\|_2 = \sum_{q=1}^{m} \hat{J}_q(\boldsymbol{\theta})^2 \tag{17}$$

$$\|\hat{\boldsymbol{J}}(\boldsymbol{\theta})\|_\infty = \max \hat{\boldsymbol{J}}(\boldsymbol{\theta}) \tag{18}$$

The LD visualization uses a two dimensional graph for every objective and every decision variable. The ordered pairs $\left(J_q(\boldsymbol{\theta}), \|\hat{\boldsymbol{J}}(\boldsymbol{\theta})\|_p\right)$ in each objective sub-graph and $\left(\theta_l, \|\hat{\boldsymbol{J}}(\boldsymbol{\theta})\|_p\right)$ in each decision variable sub-graph are plotted. Therefore, a given solution will have the same y-value in all graphs (see Figure 4). This correspondence will help to evaluate general tendencies along the Pareto front and compare solutions according to the selected norm. For example, an euclidian norm is helpful to evaluate the distance of a given solution with respect to the ideal solution, meanwhile a maximum norm will give information about the trade-off achieved by this solution. Using a norm to visualize tendencies in the Pareto front does not deform the MOP essence, since this visualization process take place after the optimization stage.

In all cases, the lower the norm, the closer to the ideal solution $\boldsymbol{J}^{min}$. For example, in figure 4, point A is the closest solution to $\boldsymbol{J}^{min}$ with the $\|\cdot\|_1$ norm. This does not mean that point A

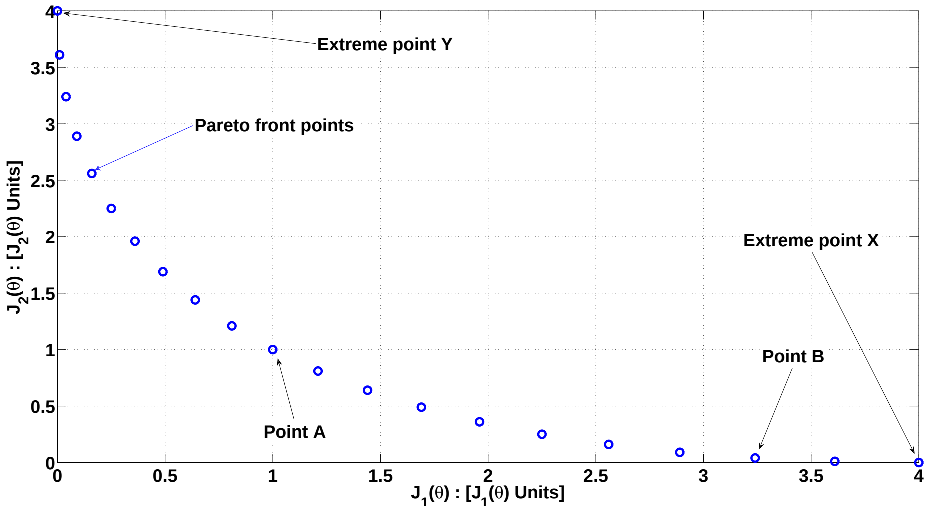

(a) Typical visualization of the Pareto front for bi-objective problems.

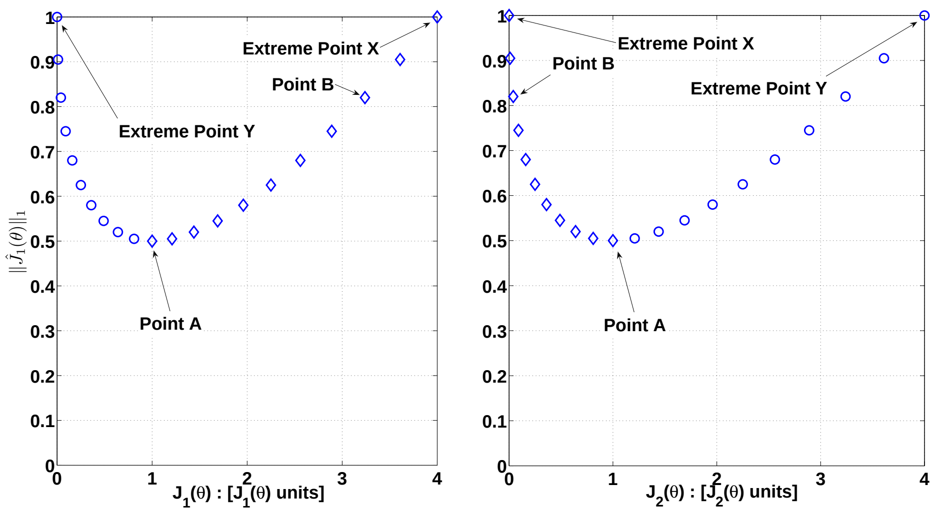

(b) Representation using LD visualization.

Fig. 4: LD visualization. Points at the same level in LD correspond on each graphic.

must be selected by the DM. Selection will be performed according with the visual information from the LD visualization and the DM preferences. In the same figure, it is possible to visualize how the tradeoff rate changes in solution A. That is, it is possible to appreciate two different tendencies around solution A: in one hand, the better $J_2(\boldsymbol{\theta})$ value, the worst $J_1(\boldsymbol{\theta})$ value (circles). In the other hand, the worst $J_2(\boldsymbol{\theta})$ value, the better $J_1(\boldsymbol{\theta})$ value (diamonds). It is difficult to appreciate such tendencies with classical visualizations with more than three objectives. For the remainder of this paper, the $\|\cdot\|_2$ norm will be used.

The LD visualization also enables the comparison of Pareto fronts obtained for different design concepts [53] (in this case, controller schemes). In such visualization, it will be possible to analyze the different trade-offs achieved by different control solutions, and determine under which circumstances it is justified to use one over another. For example, in figure 5, it is possible to see how a PID can achieve a better trade-off than a PI controller between load rejection and step setpoint change (Zone Y). In the same way, it is possible to determine under which conditions performance will be the same (Zone W).

To plot the LD, the LD visualization tool (LD-tool) [6] will be used. This is *a posteriori* visualization tool (*i.e.* is used after the optimization process) and enables the DM to identify preferences zones along the Pareto front, as well as selecting and comparing solutions. With this tool, it is possible to remove objectives or to add new performance measurements, not used in the optimization stage. Furthermore, it is possible to integrate the DM preferences in a lexicographic environment (as the one proposed by physical programming) to identify preferred solutions.

The aforementioned steps (problem definition, MOO process and the decision making stage) are important to guarantee the overall design methodology. With a poor problem definition, not matter how good our MOEA and decision making methodologies are, we will not have solutions which guarantee a good performance on the real system. If the MOEA have a low performance, the DM will not have a useful Pareto set to analyze and select a solution according with his/her preferences. Finally, a lack of decision making tools and methodologies imply a lower degree of embedment of the DM into the solution selection and tradeoff impacts. Furthermore it could lead the DM to a lack of interest in the MOO approach.

IV. EXPERIMENTAL VALIDATION OF THE MOOD4CT PROCEDURE

To show the applicability of the method, two different approaches of controller tuning for a non-linear twin rotor MIMO system (TRMS) are presented.

The TRMS is an academic workbench and a useful platform to evaluate control strategies [54]–[56] due to its complexity, non-linearities, and inaccessibility of states. It is a TITO (two inputs, two outputs) system, where two DC motors have control over the vertical angle (main

[6] Available at http://www.mathworks.com/matlabcentral/fileexchange/24042

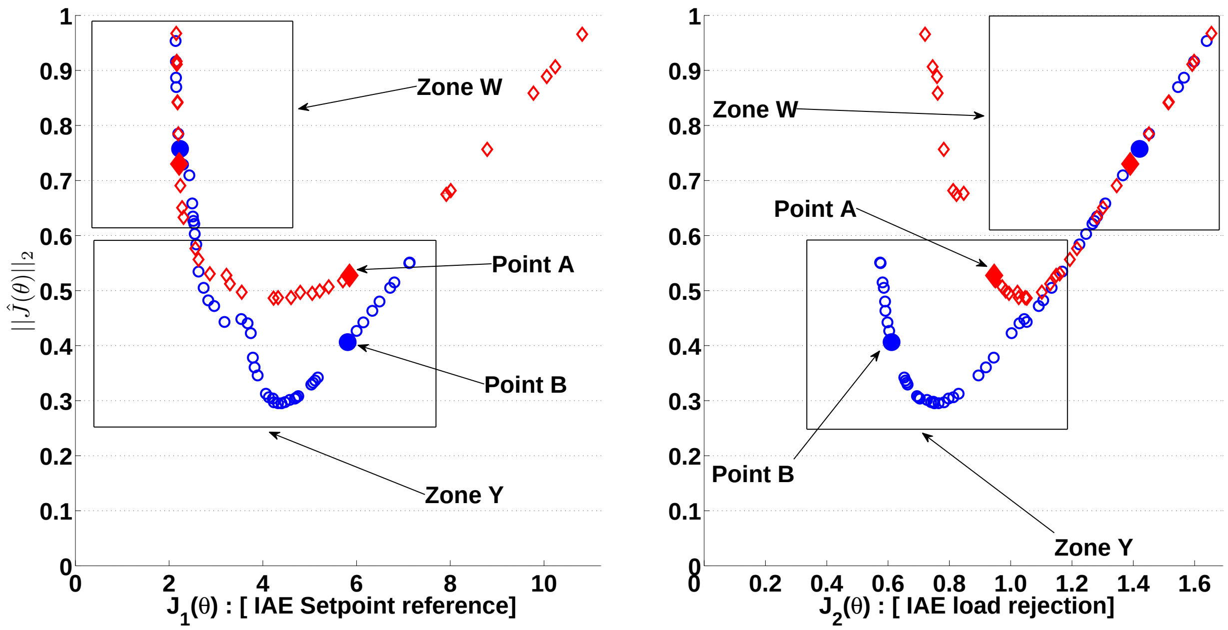

Fig. 5: Typical LD comparison for a SISO using a PI (◊) and a PID controller (◯).

angle) and horizontal angle (tail angle) respectively. Both inputs are limited in the normalized range ± 1, the main angle being in the range $[-0.5, 0.5]$ rad. And the tail angle in $[-3.0, 3.0]$ rad.

The *mood4ct* procedure is validated in two steps:

1) An optimization stage using an identified process model to obtain $\mathbf{\Theta}_P^*, \boldsymbol{J}_P^*$.
2) An experimental validation of the MOO results $\mathbf{\Theta}_P^*, \boldsymbol{J}_P^*$ on the real TRMS.

A. Optimization stage

A non-linear state-space model was identified as a part of the controller tuning-design procedure. Details on the system modeling and the observer design can be consulted in [57] and Appendix A.

To evaluate the performance of a given controller a Simulink© model with the identified non-linear model was used. Two simulations were carried out with different patterns:

- Simulation pattern 1: Setpoint step change for main from 0 rad to 0.4 rad while tail setpoint is maintained at 0.

- Simulation pattern 2: Setpoint step change for tail from 0 rad to 2.4 rad while main setpoint is maintained at 0.

The objectives defined in equations (6), (7), (9) and (10) are used according to a TITO system:

$$J_{\mathcal{E}}^{TITO}(\boldsymbol{\theta}) = T_s \begin{bmatrix} \max\left(\frac{IAE^{1,1}(\boldsymbol{\theta})}{\Delta R^1}, \frac{IAE^{2,2}(\boldsymbol{\theta})}{\Delta R^2}\right) \\ \min\left(\frac{IAE^{1,1}(\boldsymbol{\theta})}{\Delta R^1}, \frac{IAE^{2,2}(\boldsymbol{\theta})}{\Delta R^2}\right) \end{bmatrix}^T \times \boldsymbol{w} \tag{19}$$

$$J_{\mathcal{U}}^{TITO}(\boldsymbol{\theta}) = \begin{bmatrix} \max\left(\sum_{j=1}^{2} \frac{IADU^{1,j}(\boldsymbol{\theta})}{\Delta U^1_{max}}, \sum_{j=1}^{2} \frac{IADU^{2,j}(\boldsymbol{\theta})}{\Delta U^2_{max}}\right) \\ \min\left(\sum_{j=1}^{2} \frac{IADU^{1,j}(\boldsymbol{\theta})}{\Delta U^1_{max}}, \sum_{j=1}^{2} \frac{IADU^{2,j}(\boldsymbol{\theta})}{\Delta U^2_{max}}\right) \end{bmatrix}^T \times \boldsymbol{w} \tag{20}$$

$$J_{\mathcal{C}}^{TITO}(\boldsymbol{\theta}) = T_s \begin{bmatrix} \max\left(\frac{IAE^{1,2}(\boldsymbol{\theta})}{\Delta R^1_{max}}, \frac{IAE^{2,1}(\boldsymbol{\theta})}{\Delta R^2_{max}}\right) \\ \min\left(\frac{IAE^{1,2}(\boldsymbol{\theta})}{\Delta R^1_{max}}, \frac{IAE^{2,1}(\boldsymbol{\theta})}{\Delta R^2_{max}}\right) \end{bmatrix}^T \times \boldsymbol{w} \tag{21}$$

Where $\boldsymbol{w}$ is set to $\boldsymbol{w} = [10^0, 10^{-1}]$. To evaluate $J_{\mathcal{T}}(\boldsymbol{\theta})$ a linearized model is used. As a weighting function for the robustness objective, the transfer function $W(s) = \frac{0.7s+2}{s+1.1}$ will be used.

With the *mood4ct* approach, any kind of controller can be tuned. In this work, two schemes are used: an ISA-PID controller [58] and a state-space controller (see figures 6 and 7). For both cases, the controller is required to work with a sampling time of 20/1000 seconds with a saturated control signal in the normalized range ± 1.

1) PID controller tuning: PID controllers currently represent a reliable digital control solution due to their simplicity. They are often used in industrial applications and so there is ongoing research into new techniques for robust PID controller tuning [59]–[63]. For this reason, the PID scheme will be the first to be evaluated.

A two degrees of freedom ISA-PID controller with a derivative filter and an anti-windup scheme will be used:

$$\begin{aligned} U(s) &= K_c\left(b + \frac{1}{T_i s} + c\frac{T_d}{T_d/Ns+1}\right)R(s) \\ &- K_c\left(1 + \frac{1}{T_i s} + \frac{T_d}{T_d/Ns+1}\right)Y(s) \end{aligned} \tag{22}$$

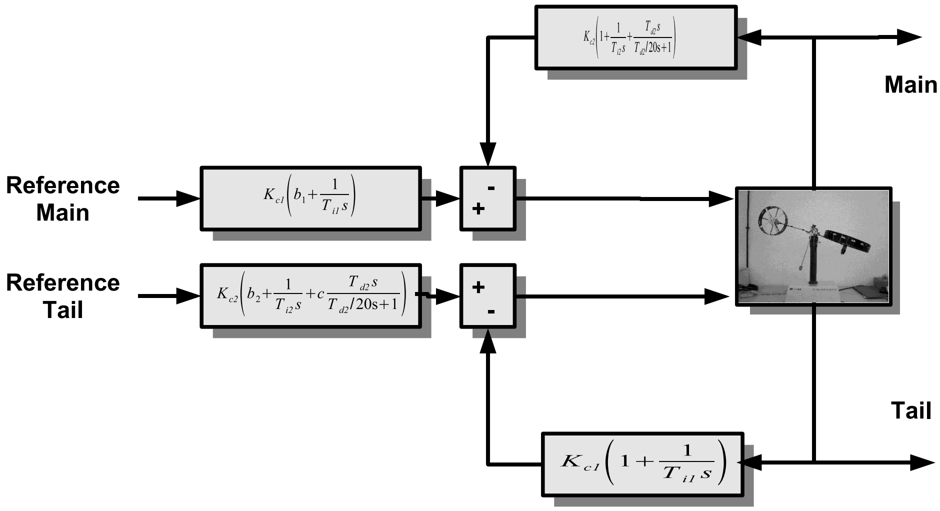

Fig. 6: PID controller scheme.

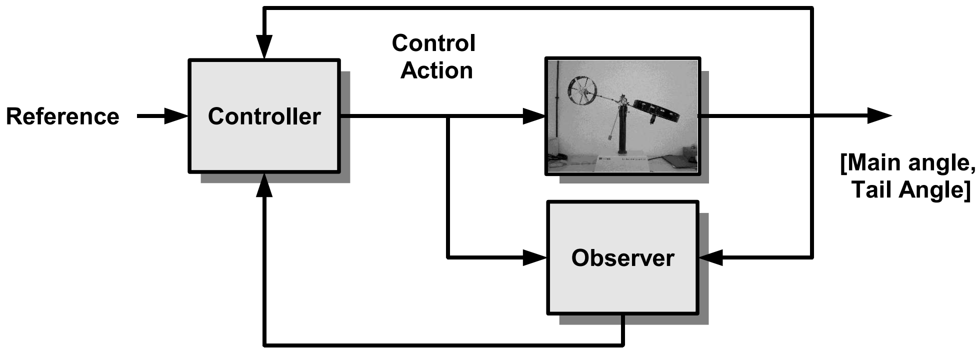

Fig. 7: State space controller proposal.

where

K_c	is the proportional gain.
T_i	represents the integral time (secs).
T_d	is the derivative time (secs).
N	represents the derivative filter. Common values for this filter lie in the range $N = [3, 20]$.
b	is the setpoint weighting for the proportional action.
c	is the setpoint weighting for the derivative action.

The antiwind-up is performed by conditional integration when the output signal is saturated [64]. The strategy to be implemented is a PI controller for the main angle and a PID controller for the tail angle. A setpoint weighting for the derivative action of $c = 0$ and a derivative filter of

TABLE I: MOO statement for the PID controller approach.

$\min_{\boldsymbol{\theta}\in\Re^7} \boldsymbol{J}(\boldsymbol{\theta}) \in \Re^5$		
$J_{\mathcal{E}}(\boldsymbol{\theta}) =$	$T_s\left[\max\left(\frac{IAE_{step}^{Main}}{0.4}, \frac{IAE_{step}^{Tail}}{2.4}\right) + 10^{-2}\min\left(\frac{IAE_{step}^{Main}}{0.4}, \frac{IAE_{step}^{Tail}}{2.4}\right)\right]$	$K_{c1,c2} \in [0,1]$
$J_{\mathcal{U}}(\boldsymbol{\theta}) =$	$\max\left(\sum \Delta u_{step}^{Main} + \sum \Delta u_{pert}^{Main}, \sum \Delta u_{step}^{Tail} + \sum \Delta u_{pert}^{Tail}\right)+$ $10^{-2}\min\left(\sum \Delta u_{step}^{Main} + \sum \Delta u_{pert}^{Main}, \sum \Delta u_{step}^{Tail} + \sum \Delta u_{pert}^{Tail}\right)$	$T_{i1,i2} \in (0,100]$
$J_{\mathcal{C}}(\boldsymbol{\theta}) =$	$T_s\left[\max\left(\frac{IAE_{pert}^{Main}}{(2\cdot 0.5)}, \frac{IAE_{pert}^{Tail}}{(2\cdot 3)}\right) + 10^{-2}\min\left(\frac{IAE_{pert}^{Main}}{(2\cdot 0.5)}, \frac{IAE_{pert}^{Tail}}{(2\cdot 3)}\right)\right]$	$T_{d2} \in [0,10]$
$J_{\mathcal{I}}(\boldsymbol{\theta}) =$	$\sup_{\omega} \bar{\sigma}\left(\mathcal{S}(\jmath\omega)\right), \omega \in (10^{-2}, 10^2)$	$b_{1,2} \in [0,1]$
$J_{\mathcal{T}}(\boldsymbol{\theta}) =$	$\sup_{\omega} \bar{\sigma}\left(\mathcal{T}(\jmath\omega)W(\jmath\omega)\right), \omega \in (10^{-2}, 10^2), s.t. J_5 > 0.8$	

$N = 20$ will also be used. Therefore, the *mood4ct* approach will be used to adjust the parameters K_{c1}, T_{i1}, b_1 for the PI controller and K_{c2}, T_{i2}, b_2 and T_d for the PID controller. Both will be tuned under SISO design considerations.

A total of five objectives are defined (see Table I). $J_{\mathcal{E}}(\boldsymbol{\theta})$, $J_{\mathcal{U}}(\boldsymbol{\theta})$, $J_{\mathcal{C}}(\boldsymbol{\theta})$, and $J_{\mathcal{T}}(\boldsymbol{\theta})$ are defined according to equations (19), (20), (21) and (10) respectively. Objective $J_{\mathcal{I}}(\boldsymbol{\theta})$ is included to prefer controllers with better disturbance rejection.

The $\boldsymbol{\Theta}_P^*$ and $\boldsymbol{J}_P^*$ from the *mood4ct* approach for PID tuning[7] are shown in Figure 8. A total of 471 non-dominated controllers were found (a controllers subset Gk_{1i} is identified for further analysis). The following geometrical remarks (GR) on the level diagrams and their corresponding control remarks (CR) can be seen in Figure 8:

GR 1: It can be observed that two different subsets of solutions appear when solutions with

[7]A random search with the same number of function evaluations used by the MOEA was performed for comparison purposes. This approach calculates a Pareto front approximation with 161 solutions. The approximation calculated by the MOEA dominates 49 solutions of the random search approach; the random search approximation does not dominate any solution of the MOEA approximation.

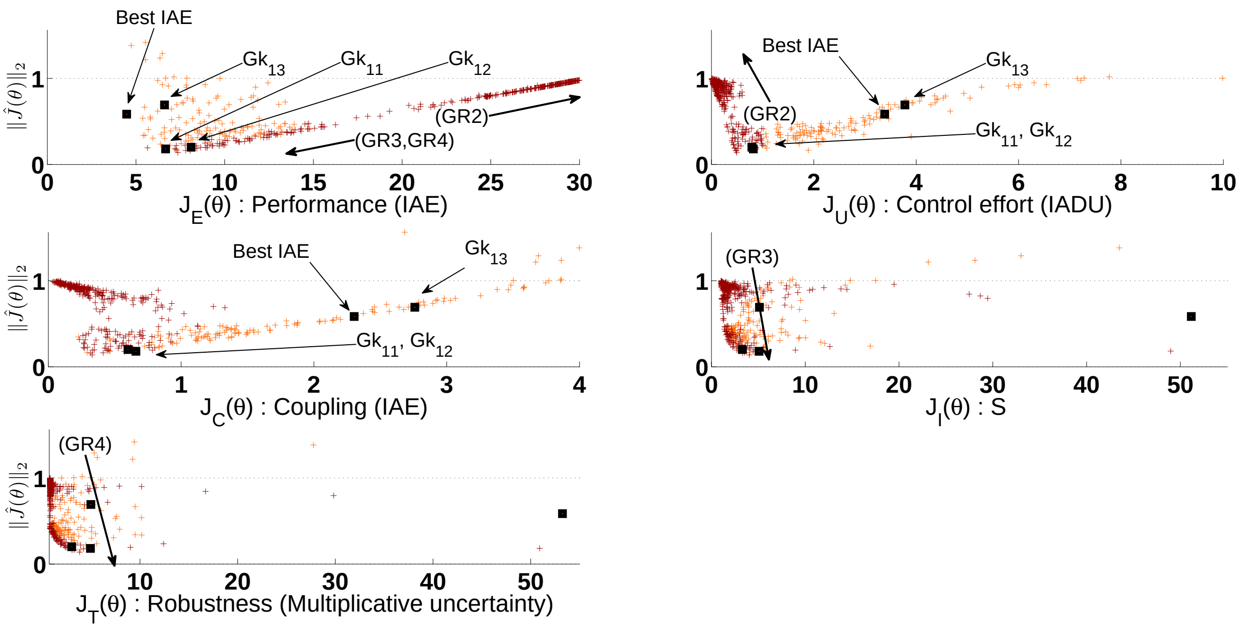

Fig. 8: $\boldsymbol{J}_P^*$ for PID controller. Dark solutions match the arbitrary requirement $J_{\mathcal{U}} \leq 1$.

$J_{\mathcal{U}}(\boldsymbol{\theta}) \leq 1$ are separated.

CR 1: The IADU performance indicator for control action is a quality indicator to differentiate damping solutions along the Pareto front.

GR 2: For solutions with $J_{\mathcal{U}}(\boldsymbol{\theta}) \leq 1$, the lower $J_{\mathcal{U}}(\boldsymbol{\theta})$, the higher $J_{\mathcal{E}}(\boldsymbol{\theta})$.

CR 2: For overdamped solutions, the higher the control effort (IADU), the better the performance (IAE).

GR 3: For solutions with $J_{\mathcal{U}}(\boldsymbol{\theta}) \leq 1$, the lower $J_{\mathcal{E}}(\boldsymbol{\theta})$, the higher $J_{\mathcal{I}}(\boldsymbol{\theta})$.

CR 3: For overdamped solutions, the better the performance (IAE), the worse the disturbance rejection ($J_{\mathcal{I}}(\boldsymbol{\theta})$).

GR 4: For solutions with $J_{\mathcal{U}}(\boldsymbol{\theta}) \leq 1$, the lower $J_{\mathcal{E}}(\boldsymbol{\theta})$, the higher $J_{\mathcal{T}}(\boldsymbol{\theta})$.

CR 4: For overdamped solutions, the better performance (IAE), the worse the robustness.

All of these points are well-known considerations in control theory. The Pareto front enables the visualization of this trade-off between objectives; and the DM can choose a solution that meets his own needs and preferences.

TABLE II: MOO statement for the state space controller approach.

$\min_{\boldsymbol{\theta} \in \Re^{16}} \boldsymbol{J}(\boldsymbol{\theta}) \in \Re^5$		
$J_{\mathcal{E}}(\boldsymbol{\theta}) =$	$T_s \left[\max \left(\frac{IAE^{Main}_{step}}{0.4}, \frac{IAE^{Tail}_{step}}{2.4} \right) + 10^{-2} \min \left(\frac{IAE^{Main}_{step}}{0.4}, \frac{IAE^{Tail}_{step}}{2.4} \right) \right]$	$\theta_i \in [-10, 10]$
$J_{\mathcal{U}}(\boldsymbol{\theta}) =$	$\max \left(\sum \Delta u^{Main}_{step} + \sum \Delta u^{Main}_{pert}, \sum \Delta u^{Tail}_{step} + \sum \Delta u^{Tail}_{pert} \right) +$ $10^{-2} \min \left(\sum \Delta u^{Main}_{step} + \sum \Delta u^{Main}_{pert}, \sum \Delta u^{Tail}_{step} + \sum \Delta u^{Tail}_{pert} \right)$	$i \in (1, 2, \ldots, 16)$
$J_{\mathcal{C}}(\boldsymbol{\theta}) =$	$T_s \left[\max \left(\frac{IAE^{Main}_{pert}}{(2 \cdot 0.5)}, \frac{IAE^{Tail}_{pert}}{(2 \cdot 3)} \right) + 10^{-2} \min \left(\frac{IAE^{Main}_{pert}}{(2 \cdot 0.5)}, \frac{IAE^{Tail}_{pert}}{(2 \cdot 3)} \right) \right]$	
$J_{\mathcal{I}}(\boldsymbol{\theta}) =$	$trace(K * K')$	
$J_{\mathcal{T}}(\boldsymbol{\theta}) =$	$\sup_{\omega} \bar{\sigma} \left(\mathcal{T}(\jmath\omega) W(\jmath\omega) \right), \omega \in (10^{-2}, 10^2), s.t. J_5 > 0.8$	

2) State space feedback controller tuning: The above proposal used a PI-PID SISO strategy to address the control of a MIMO system. Such an approach is sometimes not enough to gain satisfactory control in a wide operational working zone, mainly because of the coupling dynamics. For this reason, a matrix gain for a state space (SS) control approach is selected as a second strategy (see Figure 7).

The *mood4ct* approach will be used to adjust a feedback gain matrix $K_{2\times 8}$ to control the system. A total of five objectives are defined (see Table II). Objectives $J_{\mathcal{E}}$, $J_{\mathcal{U}}$, $J_{\mathcal{C}}$, and $J_{\mathcal{T}}$ are again defined according to equations 19, 20, 21 and 10. Objective $J_{\mathcal{I}}$ is included to have preference over controllers with lower numerical sensibility, *i.e.* well balanced controllers at the implementation stage.

The Pareto front approximation $\boldsymbol{J}^*_P$[8] is shown in Figure 9. As a result, 589 non-dominated solutions were found (a controllers subset Gk_{2i} is identified for further analysis). The following geometrical remarks (GR) and their corresponding control remarks (CR) can be seen in Figure

[8]A random search with the same number of function evaluations used by the MOEA was performed for comparison purposes. This approach calculates a Pareto front approximation with 86 solutions. The approximation calculated by the MOEA dominates 85 solutions of the random search approach; the random search approximation does not dominate any solution of the MOEA approximation.

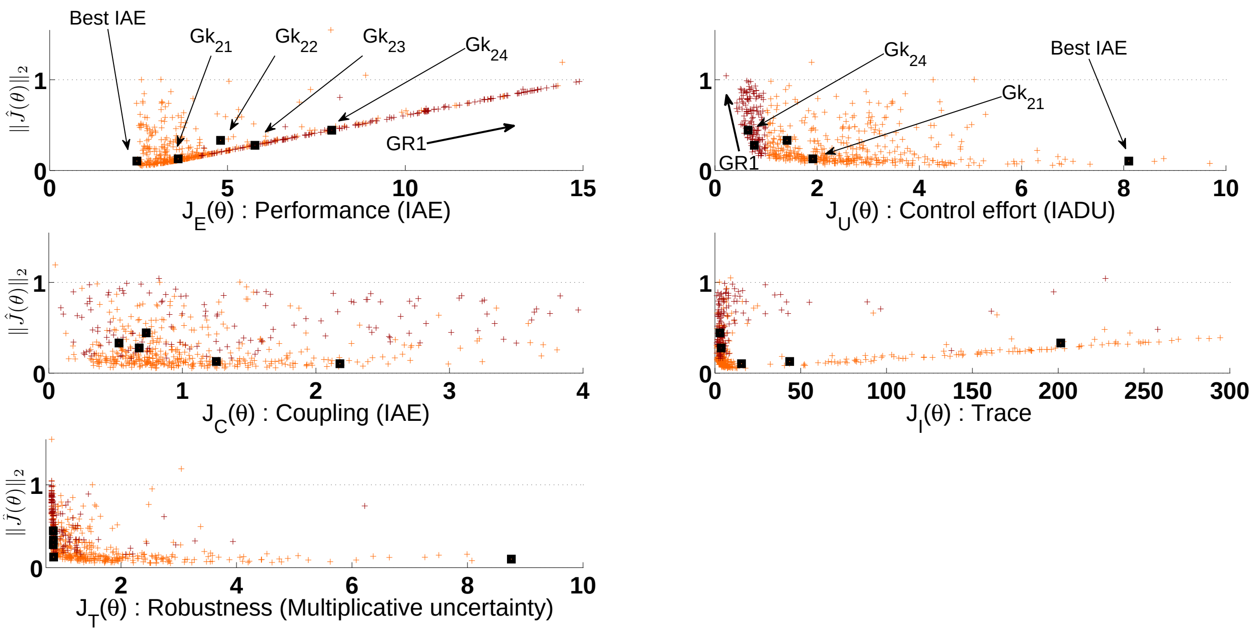

Fig. 9: $\boldsymbol{J}_P^*$ for the SS controller. Dark solutions match the arbitrary requirement $J_{\mathcal{U}}(\boldsymbol{\theta}) \leq 1$.

9:

GR 1: For solutions with $J_{\mathcal{U}} \leq 1$, the lower $J_{\mathcal{U}}(\boldsymbol{\theta})$, the higher $J_{\mathcal{E}}(\boldsymbol{\theta})$.

CR 1: For overdamped solutions, the higher the control effort (IADU), the better the performance (IAE).

GR 2: For objective $J_{\mathcal{I}}(\boldsymbol{\theta})$, solutions matching the requirement $J_{\mathcal{U}}(\boldsymbol{\theta}) \leq 1$ have the lower trace.

CR 2: Solutions with more balanced coefficients in the matrix gain are solutions that offer less damping responses.

B. Experimental validation

To validate both approaches, the setpoint pattern on Figure 10 is used on the real TRMS [9]. It is important to note that such a pattern is different from the one used at the optimization stage. In this way, it will be possible to evaluate and validate the *mood4ct* approach. The new

[9]Controllers from Tables III and VI were implemented in a National Instruments PXI-1002 System.

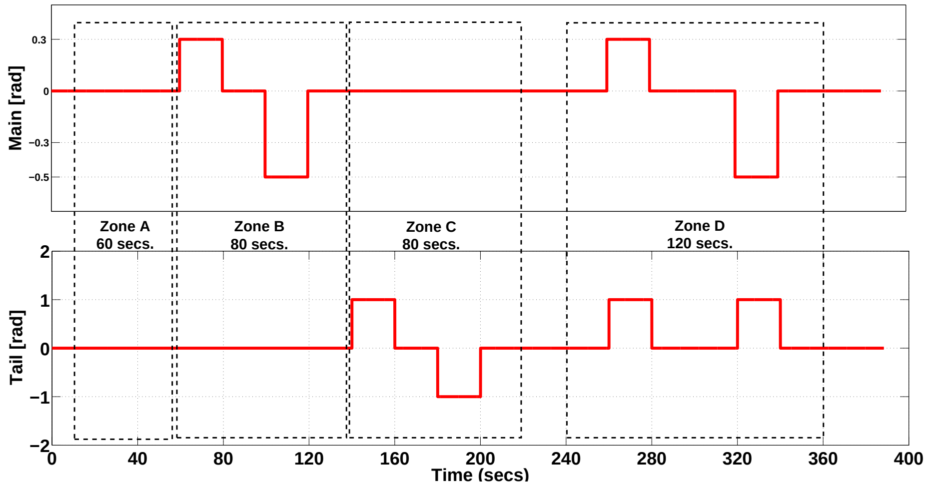

Fig. 10: Pattern for test on real TRMS. Idle state value for the main angle is around 0.3 rad.

pattern evaluates the performance of a given controller in maintaining zero-reference (zone A); a setpoint change in the main angle (zone B); a setpoint change in the tail position (zone C); and simultaneous changes in reference (zone D).

1) PID controller - experimental results: A subset of three controllers (see Table III) are selected from the Pareto set (Figure 8) for further analysis on the TRMS. Controller Gk_{13} is selected due to its performance on $J_{\mathcal{E}}(\boldsymbol{\theta})$; controller Gk_{11} due to its trade-off for objectives $J_{\mathcal{U}}(\boldsymbol{\theta})$ and $J_{\mathcal{C}}(\boldsymbol{\theta})$ (some performance is sacrificed in order to obtain a better control effort and less coupling between the main and tail closed loops). Finally, controller Gk_{12} is selected due to its robustness (this is a controller capable of working with a larger set of plants because it has a smaller $J_{\mathcal{T}}(\boldsymbol{\theta})$ value). In all cases, it is observed that the robustness requirement $J_{\mathcal{T}}(\boldsymbol{\theta}) < 1$ is not achieved. The reason for this could be: 1) it is not possible to use a PID scheme to control the system; or 2) the weighting function for robustness has not been chosen correctly (*i.e.* it is an excessive constraint) and the control engineer needs to evaluate if this constraint could be relaxed. After some analysis on the closed loop frequency response, it is determined that it is possible to use these controllers in a small operation range. The performances of these controllers with the reference pattern for the real test (see Figure 10) are shown in Tables IV, V and Figure 11.

As expected, controller Gk_{12} had the worst performance, but fewer coupling effects and the

TABLE III: PID controllers selected from Θ_P^* (Figure 8).

	$J_{\mathcal{E}}(\boldsymbol{\theta})$	$J_{\mathcal{U}}(\boldsymbol{\theta})$	$J_{\mathcal{C}}(\boldsymbol{\theta})$	$J_{\mathcal{I}}(\boldsymbol{\theta})$	$J_{\mathcal{T}}(\boldsymbol{\theta})$	$\boldsymbol{\theta} = (K_{c1}, T_{i1}, b_1, K_{c2}, T_{i2}, T_{d2}, b_2)$
Gk_{11}	6.83	0.82	0.65	4.76	4.58	$\boldsymbol{\theta} = (0.001, 0.006, 0.99, 0.269, 8.258, 1.420, 0.626)$
Gk_{12}	8.60	0.79	0.59	2.94	2.61	$\boldsymbol{\theta} = (0.001, 0.008, 0.68, 0.2533, 8.45, 1.14, 0.84)$
Gk_{13}	6.81	3.76	2.74	4.76	4.58	$\boldsymbol{\theta} = (0.001, 0.006, 0.70, 0.999, 7.396, 1.887, 0.6721)$

TABLE IV: Performance of PI-PID controllers on the real TRMS (Zones A and B)

<table>
<tr><th colspan="5">Zone A</th></tr>
<tr><th></th><th></th><th>IAE</th><th>IADU</th><th>Obj</th></tr>
<tr><td rowspan="3">Gk_{11}</td><td>Main</td><td>4.76E+000</td><td>2.85E-002</td><td>$J_1 = 1.31E-001$</td></tr>
<tr><td>Tail</td><td>1.07E+001</td><td>4.67E+000</td><td>$\boldsymbol{J_2 = 4.67E+000}$</td></tr>
<tr><td></td><td>—</td><td>—</td><td>$J_3 = -----$</td></tr>
<tr><td rowspan="3">Gk_{12}</td><td>Main</td><td>6.45E+000</td><td>3.05E-002</td><td>$J_1 = 2.43E-001$</td></tr>
<tr><td>Tail</td><td>3.42E+001</td><td>4.81E+000</td><td>$J_2 = 4.81E+000$</td></tr>
<tr><td></td><td>—</td><td>—</td><td>$J_3 = -----$</td></tr>
<tr><td rowspan="3">Gk_{13}</td><td>Main</td><td>3.58E+000</td><td>2.03E-002</td><td>$J_1 = 9.89E-002$</td></tr>
<tr><td>Tail</td><td>8.17E+000</td><td>1.65E+001</td><td>$\boldsymbol{J_2 = 1.65E+001}$</td></tr>
<tr><td></td><td>—</td><td>—</td><td>$J_3 = -----$</td></tr>
<tr><th colspan="5">Zone B</th></tr>
<tr><th></th><th></th><th>IAE</th><th>IADU</th><th>Obj</th></tr>
<tr><td rowspan="3">Gk_{11}</td><td>Main</td><td>3.73E+002</td><td>2.23E+000</td><td>$\boldsymbol{J_1 = 2.49E+001}$</td></tr>
<tr><td>Tail</td><td>1.14E+003</td><td>5.74E+001</td><td>$\boldsymbol{J_2 = 5.74E+001}$</td></tr>
<tr><td></td><td>—</td><td>—</td><td>$J_3 = 3.81E+000$</td></tr>
<tr><td rowspan="3">Gk_{12}</td><td>Main</td><td>4.44E+002</td><td>2.11E+000</td><td>$J_1 = 2.96E+001$</td></tr>
<tr><td>Tail</td><td>1.27E+003</td><td>5.91E+001</td><td>$J_2 = 5.91E+001$</td></tr>
<tr><td></td><td>—</td><td>—</td><td>$J_3 = 4.24E+000$</td></tr>
<tr><td rowspan="3">Gk_{13}</td><td>Main</td><td>3.86E+002</td><td>2.20E+000</td><td>$J_1 = 2.57E+001$</td></tr>
<tr><td>Tail</td><td>3.12E+002</td><td>1.80E+002</td><td>$J_2 = 1.80E+002$</td></tr>
<tr><td></td><td>—</td><td>—</td><td>$\boldsymbol{J_3 = 1.04E+000}$</td></tr>
</table>

TABLE V: Performance of the PI-PID controllers on the real TRMS (Zones C and D)

		IAE	IADU	Obj
Zone C				
Gk_{11}	Main	5.68E+001	3.45E-001	$J_1 = 1.13E + 001$
	Tail	5.65E+002	4.26E+001	$J_2 = 4.26E + 001$
		—	—	$\boldsymbol{J_3 = 1.14E + 000}$
Gk_{12}	Main	5.71E+001	2.74E-001	$J_1 = 1.28E + 001$
	Tail	6.42E+002	3.87E+001	$\boldsymbol{J_2 = 3.87E + 001}$
		—	—	$\boldsymbol{J_3 = 1.14E + 000}$
Gk_{13}	Main	6.36E+001	3.69E-001	$\boldsymbol{J_1 = 8.64E + 000}$
	Tail	4.32E+002	1.21E+002	$J_2 = 1.21E + 002$
		—	—	$J_3 = 1.27E + 000$
Zone D				
Gk_{11}	Main	3.97E+002	2.36E+000	$J_1 = 5.48E + 001$
	Tail	1.41E+003	7.45E+001	$J_2 = 7.45E + 001$
		—	—	$J_3 = - - - - -$
Gk_{12}	Main	6.03E+002	1.97E+000	$J_1 = 7.76E + 001$
	Tail	1.87E+003	6.34E+001	$\boldsymbol{J_2 = 6.34E + 001}$
		—	—	$J_3 = - - - - -$
Gk_{13}	Main	3.88E+002	2.19E+000	$\boldsymbol{J_1 = 3.70E + 001}$
	Tail	5.57E+002	2.24E+002	$J_2 = 2.24E + 002$
		—	—	$J_3 = - - - - -$

best control effort on zones C and D. Controller Gk_{13}, as indicated by the Pareto front, has the highest control effort in all cases and the best performance on zones A and D. Finally, controller Gk_{11} presents a good trade-off between performance and control effort.

2) State space approach - experimental results: A subset of six controllers (Table VI) was selected from the Pareto set (Figure 9), according to the control requirements and the closed loop frequency response on the linear model. Notice that it is possible to fulfill the requirement $J_{\mathcal{T}}(\boldsymbol{\theta}) < 1$, meaning that a larger set of plants can be controlled by the state space approach. Controller Gk_{21} is selected because it is the controller with the lowest 2-norm on the level diagram, while controller Gk_{22} is selected to analyze the impact of $J_{\mathcal{I}}(\boldsymbol{\theta})$ on performance. Controllers Gk_{23} and Gk_{24} are selected to validate the trade-off achieved by decreasing the

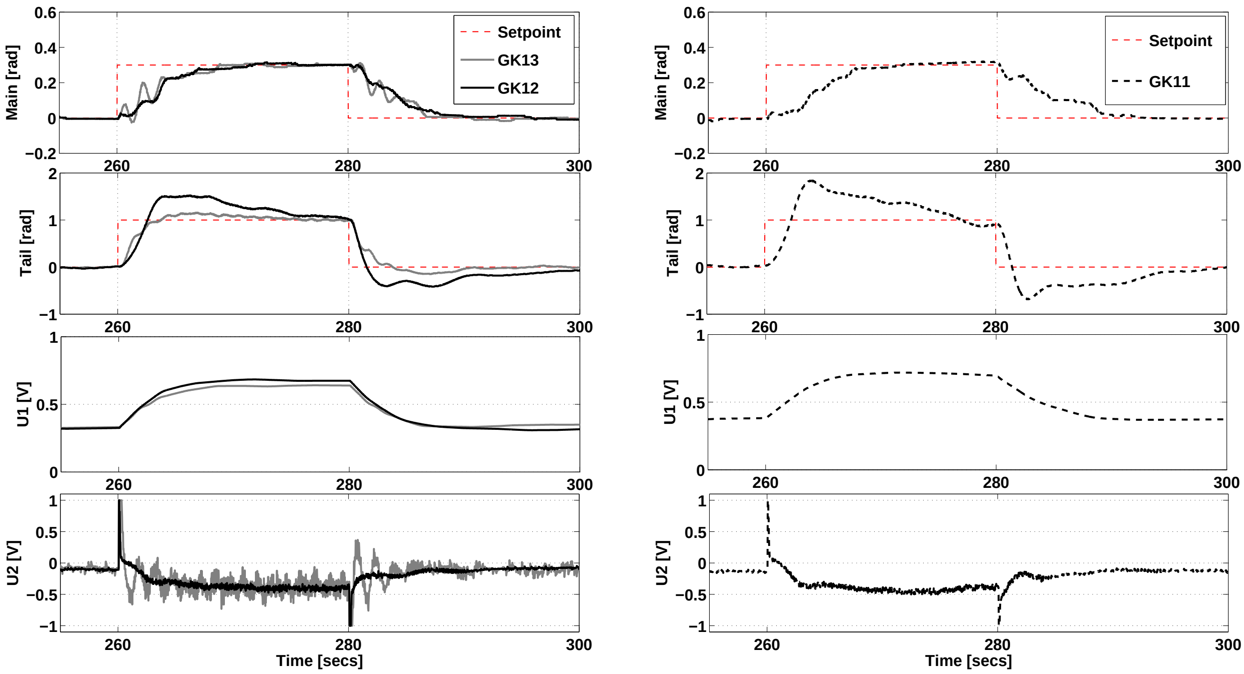

Fig. 11: Performance on the real TRMS of the *mood4ct*-PID approach for the setpoint pattern.

performance in order to gain a better control action and less coupling effects between the main and tail angles. The performance of these controllers with the reference step pattern for the real test (see Figure 10) is shown in Tables VII, VIII and in Figure 12.

TABLE VI: State space controller and their performances at the optimization stage.

	$J_{\mathcal{E}}(\boldsymbol{\theta})$	$J_{\mathcal{U}}(\boldsymbol{\theta})$	$J_{\mathcal{C}}(\boldsymbol{\theta})$	$J_{\mathcal{I}}(\boldsymbol{\theta})$	$J_{\mathcal{T}}(\boldsymbol{\theta})$
Gk_{21}	3.61	1.91	1.25	43.58	0.83
Gk_{22}	4.82	1.41	0.53	201.52	0.83
Gk_{23}	5.77	0.77	0.68	3.67	0.83
Gk_{24}	7.93	0.65	0.71	2.96	0.83

Gk_{21} and Gk_{22} are controllers with outstanding performance at the expense of high control efforts ($J_{\mathcal{U}}(\boldsymbol{\theta})$) and larger trace values ($J_{\mathcal{I}}(\boldsymbol{\theta})$). Controller Gk_{21} exhibits more coupling effects as was pointed by $J_{\mathcal{C}}(\boldsymbol{\theta})$, and noise sensitivity ($J_{\mathcal{I}}(\boldsymbol{\theta})$). Controller Gk_{22} exhibits a better performance than Gk_{21} due to coupling effects ($J_{\mathcal{C}}(\boldsymbol{\theta})$), but also shows a higher noise control effort ($J_{\mathcal{I}}(\boldsymbol{\theta})$).

Controller Gk_{23} and Gk_{24} has almost the same performance for objectives $J_{\mathcal{U}}(\boldsymbol{\theta})$, $J_{\mathcal{C}}(\boldsymbol{\theta})$,

$J_{\mathcal{I}}(\boldsymbol{\theta})$, $J_{\mathcal{T}}(\boldsymbol{\theta})$ and it is possible to see the tradeoff predicted by the Pareto front approximation. Controller Gk_{24} shows worse performance than controller Gk_{23}, but with less control effort.

TABLE VII: Performance of the state space controller on the real TRMS (Zones A and B).

		Zone A		
		IAE	IADU	Obj
Gk_{21}	Main	8.64E+000	3.07E+001	$J_1 = 2.18E-001$
	Tail	1.36E+001	2.17E+001	$J_2 = 3.07E+001$
		—	—	$J_3 = ------$
Gk_{22}	Main	6.47E+000	7.71E+001	$\boldsymbol{J_1 = 1.88E-001}$
	Tail	1.74E+001	2.90E+001	$J_2 = 7.71E+001$
		—	—	$J_3 = -----$
Gk_{23}	Main	9.96E+000	7.94E+000	$J_1 = 2.79E-001$
	Tail	2.39E+001	8.61E+000	$J_2 = 8.61E+000$
		—	—	$J_3 = -----$
Gk_{24}	Main	9.67E+000	6.71E+000	$J_1 = 2.66E-001$
	Tail	2.19E+001	5.11E+000	$\boldsymbol{J_2 = 6.71E+000}$
		—	—	$J_3 = -----$
		Zone B		
		IAE	IADU	Obj
Gk_{21}	Main	2.53E+002	1.61E+002	$J_1 = 1.69E+001$
	Tail	1.63E+002	1.24E+002	$J_2 = 1.61E+002$
		—	—	$\boldsymbol{J_3 = 5.42E-001}$
Gk_{22}	Main	2.11E+002	4.18E+002	$\boldsymbol{J_1 = 1.40E+001}$
	Tail	3.46E+002	1.59E+002	$J_2 = 4.18E+002$
		—	—	$J_3 = 1.15E+000$
Gk_{23}	Main	3.17E+002	4.85E+001	$J_1 = 2.11E+001$
	Tail	3.28E+002	5.72E+001	$J_2 = 5.72E+001$
		—	—	$J_3 = 1.09E+000$
Gk_{24}	Main	5.79E+002	4.33E+001	$J_1 = 3.86E+001$
	Tail	3.28E+002	3.56E+001	$\boldsymbol{J_2 = 4.33E+001}$
		—	—	$J_3 = 1.09E+000$

TABLE VIII: Performance of the state space controller on the real TRMS (Zones C and D).

Zone C				
		IAE	IADU	Obj
Gk_{21}	Main	1.34E+002	1.57E+002	$\boldsymbol{J_1 = 1.01E + 001}$
	Tail	5.07E+002	1.10E+002	$J_2 = 1.57E + 002$
		—	—	$J_3 = 2.67E + 000$
Gk_{22}	Main	4.86E+001	4.02E+002	$J_1 = 1.25E + 001$
	Tail	6.26E+002	1.58E+002	$J_2 = 4.02E + 002$
		—	—	$\boldsymbol{J_3 = 9.73E - 001}$
Gk_{23}	Main	6.77E+001	3.70E+001	$J_1 = 1.04E + 001$
	Tail	5.20E+002	4.23E+001	$J_2 = 4.23E + 001$
		—	—	$J_3 = 1.35E + 000$
Gk_{24}	Main	1.06E+002	3.09E+001	$J_1 = 1.46E + 001$
	Tail	7.28E+002	2.52E+001	$\boldsymbol{J_2 = 3.09E + 001}$
		—	—	$J_3 = 2.12E + 000$
Zone D				
		IAE	IADU	Obj
Gk_{21}	Main	2.90E+002	2.25E+002	$J_1 = 3.01E + 001$
	Tail	5.34E+002	1.64E+002	$J_2 = 2.25E + 002$
		—	—	$J_2 = - - - - -$
Gk_{22}	Main	2.18E+002	6.37E+002	$\boldsymbol{J_1 = 2.96E + 001}$
	Tail	7.54E+002	2.48E+002	$J_2 = 6.37E + 002$
		—	—	$J_3 = - - - - -$
Gk_{23}	Main	3.42E+002	4.99E+001	$J_1 = 3.61E + 001$
	Tail	6.64E+002	5.51E+001	$J_2 = 5.51E + 001$
		—	—	$J_3 = - - - - -$
Gk_{24}	Main	6.20E+002	5.15E+001	$J_1 = 6.26E + 001$
	Tail	1.06E+003	4.23E+001	$\boldsymbol{J_2 = 5.15E + 001}$
		—	—	$J_3 = - - - - -$

C. Comparison between control approaches

With the multiobjective approach and the LD tool it is possible to perform an overall comparison between both control approaches. The comparison will be not limited by using just a pair of solutions (controllers), and the whole set of controllers will be used in accordance with the quality of their performances along the Pareto front approximation.

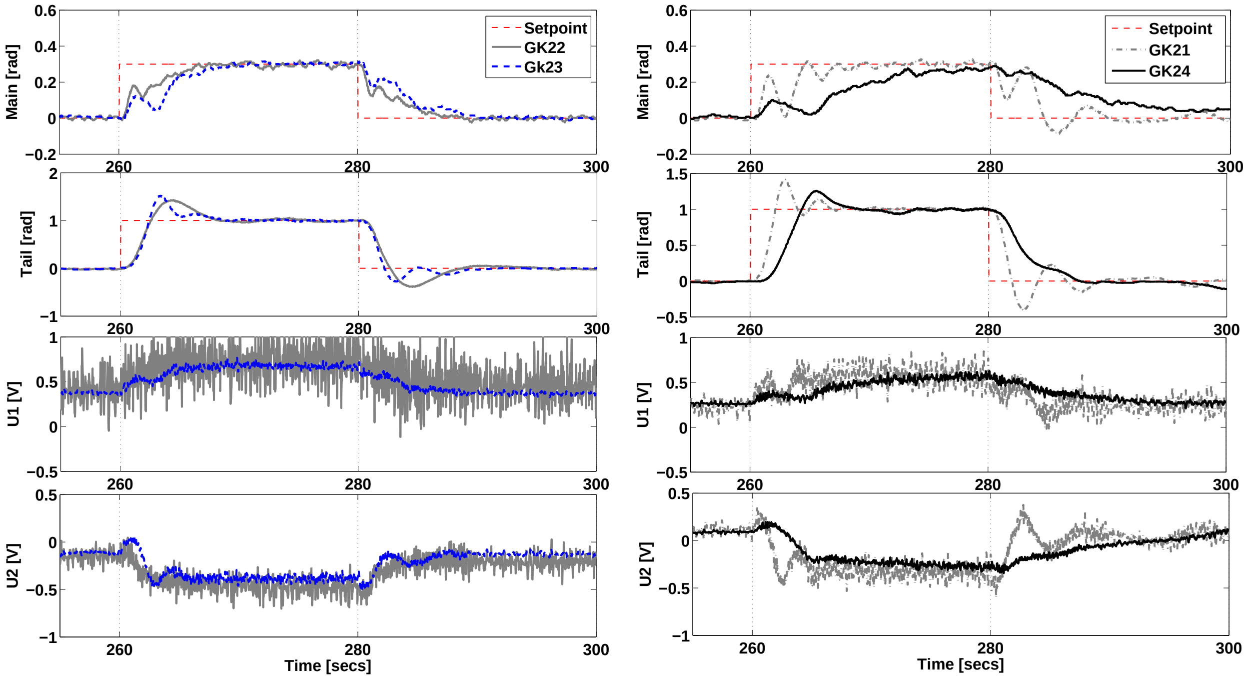

Fig. 12: Performance on the real TRMS of the *mood4ct*-SS approach on setpoint pattern.

As objective $J_{\mathcal{I}}(\boldsymbol{\theta})$ corresponds to the particular implementation of each controller, a comparison can be performed in the objective subset $\boldsymbol{J_s}(\boldsymbol{\theta}) = [J_{\mathcal{E}}(\boldsymbol{\theta}), J_{\mathcal{U}}(\boldsymbol{\theta}), J_{\mathcal{C}}(\boldsymbol{\theta}), J_{\mathcal{T}}(\boldsymbol{\theta})]$. A new level diagram, using both set of solutions (with the ideal solution being the minimal offered by two approaches) is built (see Figure 13). Again, it is possible to make some geometrical remarks (GR) and their corresponding control remarks (CR):

GR 1: In objective $J_{\mathcal{E}}$ there is a range of solutions where both approaches coincide in the LD (Zone A).

CR 1: There are configurations for each controller capable of reaching the same level of performance in the range $IAE \approx [6, 15]$.

GR 2: For the above mentioned range, solutions of the frontal state space tend to have better values in $J_{\mathcal{C}}(\boldsymbol{\theta})$ and $J_{\mathcal{T}}(\boldsymbol{\theta})$.

CR 2: For the performance range $IAE \approx [6, 15]$ the state space controller gives a better trade-off for control effort and robustness than a PID controller.

GR 3: Solutions below $\|\hat{\boldsymbol{J}}(\boldsymbol{\theta})\|_2$ (Zone B) correspond to second front solutions. These solutions tend to disperse with larger values in objectives $J_{\mathcal{U}}(\boldsymbol{\theta})$, $J_{\mathcal{C}}(\boldsymbol{\theta})$, and $J_{\mathcal{T}}(\boldsymbol{\theta})$.

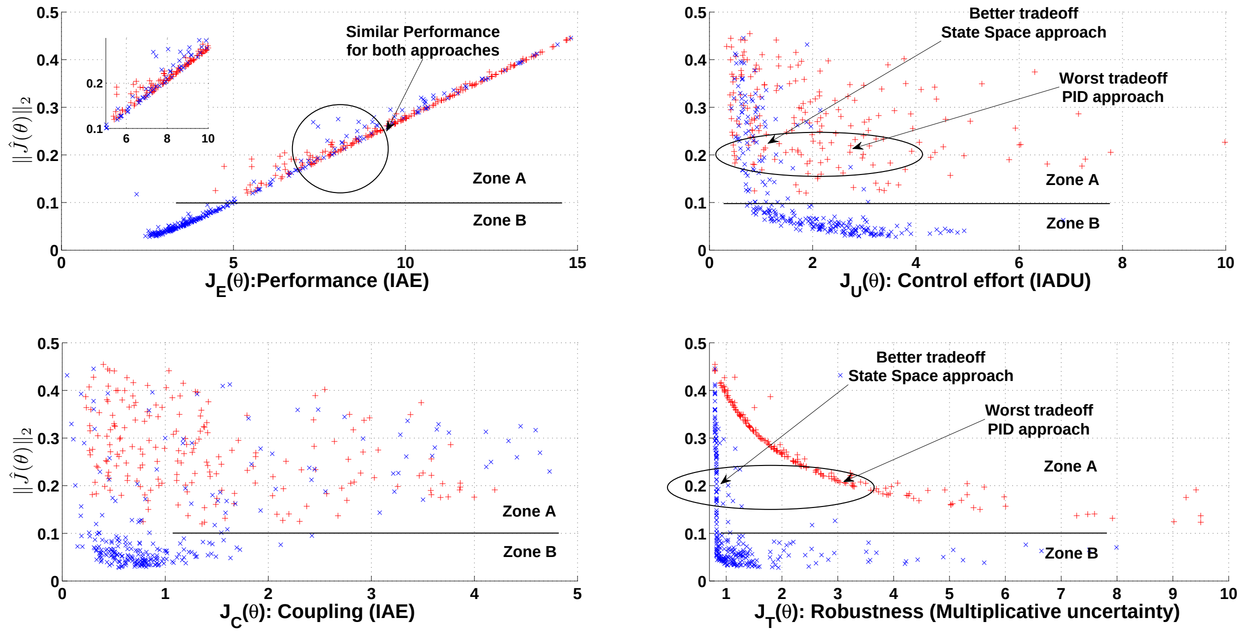

Fig. 13: Design concept comparison between: PID controllers (+) and state space controllers (x).

CR 3: The state space approach can reach closer values to the ideal solution. Nevertheless, these solutions may include the worst values for control effort, coupling effect, and robustness.

With such graphical analysis, it is possible to see the trade-off gained by using a modern control strategy such as a state space controller over a PID controller. In some instances, it will be worthwhile seeing if a complex control technique is justified over a classical technique (such as a PID controller) according with the DM preferences.

V. CONCLUSIONS

In this work, a holistic multi-objective optimisation design for controller tuning (*mood4ct*) has been presented. With *mood4ct*, it is possible to achieve a higher degree of flexibility for choosing a solution that matches the desired level of trade-off between conflicting objectives, such as performance, control effort, and robustness. The approach includes the use of meaningful performance objectives through simulation, and the use of a flexible tool to visualize m-dimensional Pareto fronts.

Mood4ct has been used to control a non-linear MIMO system. The controller tuning approach has been shown to be flexible for classical PID controllers and state space controllers tuning. It has also been shown to be reliable and robust enough to control the system with different reference patterns. This approach makes it possible to achieve a desired trade-off between performance and robustness, which leads to better implementation results on a real system than the results achievable by optimizing just a performance measurement. As the tendencies are those predicted by $\boldsymbol{J}_P^*$ from the optimization stage with the process model, the *mood4ct* procedure is validated as a tool for designing different control architectures.

Finally, using the level diagram tool a global comparison has been made between different control approaches, and this is useful to determine if a complex control technique is justified in preference to a classical technique that matches the DM preferences. Further research will focus on more interpretable objectives for robust control and stability.

APPENDIX

All models and controllers in this work are available to download (Simulink© format) from:

- http://personales.upv.es/gilreyme/mood4ct/mood4ct.html

A. State space linear model

$$\begin{pmatrix} \dot{x} = Ax + Bu \\ y = Cx \end{pmatrix}, C = \begin{bmatrix} 1 & 0 & 0 & 0 & 0 & 0 \\ 0 & 0 & 0 & 1 & 0 & 0 \end{bmatrix} \tag{23}$$

$$A = \begin{bmatrix} 0 & 1 & 0 & 0 & 0 & 0 \\ -4.74 & -0.03 & 5.66 & 0 & 0 & 0 \\ 0 & 0 & -0.75 & 0 & 0 & 0 \\ 0 & 0 & 0 & 0 & 1 & 0 \\ 0 & 0 & 0 & -0.12 & -0.19 & 1 \\ 0 & 0 & 0 & 0 & 0 & -2.33 \end{bmatrix}, B = \begin{bmatrix} 0 & 0 \\ 0 & 0.239 \\ 0.752 & 0 \\ 0 & 0 \\ 0 & 0 \\ 0 & 2.326 \end{bmatrix} \tag{24}$$

ACKNOWLEDGMENT

This work was partially supported by the FPI-2010/19 grant from the Universitat Politècnica de València and the project DPI2008-02133/DPI from the Spanish Ministry of Science and Innovation.

REFERENCES

[1] M. Garcia-Alvarado and I. Ruiz-Lopez, "A design method for robust and quadratic optimal mimo linear controllers," *Chemical Engineering Science*, vol. 65, no. 11, pp. 3431 – 3438, 2010.

[2] K. M. Miettinen, *Nonlinear multiobjective optimization*. Kluwer Academic Publishers, 1998.

[3] R. Marler and J. Arora, "Survey of multi-objective optimization methods for engineering," *Structural and multidisciplinary optimization*, no. 26, pp. 369 – 395, 2004.

[4] A. Messac, "Physical programming: effective optimization for computational design." *AIAA Journal*, vol. 34, no. 1, pp. 149 – 158, 1996.

[5] I. Das and J. Dennis, "Normal-boundary intersection: a new method for generating the pareto surface in non-linear multicriteria optimization problems," *SIAM J. Optim.*, vol. 8, pp. 631 – 657, 1998.

[6] A. Messac, A. Ismail-Yahaya, and C. Mattson, "The normalized normal constraint method for generating the pareto frontier," *Structural and multidisciplinary optimization*, no. 25, pp. 86 – 98, 2003.

[7] S. Ruzika1 and M. Wiecek, "Successive approach to compute the bounded pareto front of practical multiobjective optimization problems," *SIAM J. Optim.*, vol. 20, pp. 915 – 934, 2009.

[8] C. A. C. Coello, D. V. Veldhuizen, and G. Lamont, *Evolutionary algorithms for solving multi-objective problems*. Kluwer Academic press, 2002.

[9] C. A. C. Coello and G. B. Lamont, *Applications of Multi-Objective evolutionary algorithms*, advances in natural computation vol. 1 ed. World scientific publishing, 2004.

[10] K. Deb, A. Pratap, S. Agarwal, and T. Meyarivan, "A fast and elitist multiobjective genetic algorithm: $nsga-ii$," *IEEE Transactions on Evolutionary Computation*, vol. 6, no. 2, pp. 124 – 141, 2002.

[11] C. Fonseca and P. Fleming, "Genetic algorithms for multiobjective optimization: formulation, discussion an generalization." *Proceedings of the fifth international conference on genetic algorithms.*, pp. 416 – 423, 1993.

[12] M. Martínez, J. Herrero, J. Sanchis, X. Blasco, and S. García-Nieto, "Applied pareto multi-objective optimization by stochastic solvers," *Engineering applications of artificial intelligence*, vol. 22, pp. 455 – 465, 2009.

[13] A. G. Hernández-Díaz, L. V. Santana-Quintero, C. A. C. Coello, and J. Molina, "Pareto-adaptive ϵ-dominance," *Evolutionary Computation*, no. 4, pp. 493 – 517, 2007.

[14] G. Reynoso-Meza, "Design, coding and implementation of a multiobjective optimization algorithm based on differential evolution with spherical pruning: applications for system identification and controller tuning." Master's thesis, Universitat Politècnica de València., 2009.

[15] C. Fonseca and P. Fleming, "Multiobjective optimization and multiple constraint handling with evolutionary algorithms. i. a unified formulation," *Systems, Man and Cybernetics, Part A: Systems and Humans, IEEE Transactions on*, vol. 28, no. 1, pp. 26 – 37, jan 1998.

[16] M. Morari and J. H. Lee, "Model predictive control: past, present and future," *Computers & Chemical Engineering*, vol. 23, no. 4-5, pp. 667 – 682, 1999.

[17] P. Fleming and R. Purshouse, "Evolutionary algorithms in control systems engineering: a survey," *Control Engineering Practice*, no. 10, pp. 1223 – 1241, 2002.

[18] W. da Silva, P. Acarnley, and J. Finch, "Application of genetic algorithms to the online tuning of electric drive speed controllers," *Industrial Electronics, IEEE Transactions on*, vol. 47, no. 1, pp. 217 – 219, feb. 2000.

[19] A. Herreros, E. Baeyens, and J. R. Perán, "Design of pid-type controllers using multiobjective genetic algorithms," *ISA Transactions*, vol. 41, no. 4, pp. 457 – 472, 2002.

[20] S. Tavakoli, I. Griffin, and P. J. Fleming, "Multi-objective optimization approach to the pi tuning problem," in *Proceedings of the IEEE congress on evolutionary computation (CEC2007)*, September 2007, pp. 3165 – 3171.

[21] T.-H. Kim, I. Maruta, and T. Sugie, "Robust pid controller tuning based on the constrained particle swarm optimization," *Automatica*, vol. 44, no. 4, pp. 1104 – 1110, 2008.

[22] A. Nobakhti and H. Wang, "A simple self-adaptive differential evolution algorithm with application on the alstom gasifier," *Applied soft computing*, vol. 8, pp. 350 – 370, 2008.

[23] M. W. Iruthayarajan and S. Baskar, "Evolutionary algorithms based design of multivariable pid controller," *Expert Systems with applications*, vol. 3, no. 36, pp. 9159 – 9167, 2009.

[24] Y. Xue, D. Li, and F. Gao, "Multi-objective optimization and selection for the pi control of alstom gasifier problem," *Control Engineering Practice*, vol. 18, no. 1, pp. 67 – 76, 2010.

[25] M. W. Iruthayarajan and S. Baskar, "Covariance matrix adaptation evolution strategy based design of centralized pid controller," *Expert Systems with Applications*, vol. 37, no. 8, pp. 5775 – 5781, 2010.

[26] S.-Z. Zhao, M. W. Iruthayarajan, S. Baskar, and P. Suganthan, "Multi-objective robust pid controller tuning using two lbests multi-objective particle swarm optimization," *Information Sciences*, vol. In Press, Uncorrected Proof, pp. –, 2011.

[27] K. Tang, K. F. Man, G. Chen, and S. Kwong, "An optimal fuzzy pid controller," *IEEE Transactions on Industrial Electronics*, vol. 48, no. 4, pp. 757 – 765, 2001.

[28] P. Melin and O. Castillo, "Intelligent control of complex electrochemical systems with a neuro-fuzzy-genetic approach," *Industrial Electronics, IEEE Transactions on*, vol. 48, no. 5, pp. 951 – 955, oct. 2001.

[29] S. H. Kim, C. Park, and F. Harashima, "A self-organized fuzzy controller for wheeled mobile robot using an evolutionary algorithm," *Industrial Electronics, IEEE Transactions on*, vol. 48, no. 2, pp. 467 – 474, apr. 2001.

[30] M. Marinaki, Y. Marinakis, and G. E. Stavroulakis, "Fuzzy control optimized by pso for vibration suppression of beams," *Control Engineering Practice*, vol. 18, no. 6, pp. 618 – 629, 2010.

[31] Z. Song and A. Kusiak, "Optimization of temporal processes: A model predictive control approach," *Evolutionary Computation, IEEE Transactions on*, vol. 13, no. 1, pp. 169 –179, feb. 2009.

[32] M. Giacomán-Zarzar, R. Ramírez-Mendoza, P. Fleming, I. Griffin, and A. Molina-Cristóbal, "Robust h_∞ controller design for aircraft lateral dynamics using multiobjective optimization and genetics algorithms," *Proceedings of the 17th IFAC World Congress*, pp. 8834 – 8839, 2008.

[33] L. Wang and L.-P. Li, "Fixed-structure controller synthesis based on differential evolution with level comparison," *Evolutionary Computation, IEEE Transactions on*, vol. 15, no. 1, pp. 120 –129, feb. 2011.

[34] A. Molina-Cristóbal, I. Griffin, P. Fleming, and D. Owens, "Linear matrix inequialities and evolutionary optimization in multiobjective control," *International Journal of systems science*, vol. 37, no. 8, pp. 513 – 522, 2006.

[35] V. V. Silva, P. J. Fleming, J. Sugimoto, and R. Yokoyama, "Multiobjective optimization using variable complexity modelling for control system design," *Applied Soft Computing*, no. 8, pp. 392 – 401, 2008.

[36] R. Purshouse, C. Jalba, and P. Fleming, "Preference-driven co-evolutionary algorithms show promise for many-objective

optimisation," in *Evolutionary Multi-Criterion Optimization*, ser. Lecture Notes in Computer Science, R. Takahashi, K. Deb, E. Wanner, and S. Greco, Eds. Springer Berlin / Heidelberg, 2011, vol. 6576, pp. 136 – 150, 10.1007/978-3-642-19893-9 10.

[37] D. Brockhoff and E. Zitzler, "Objective reduction in evolutionary multiobjective optimization: Theory and applications," *Evolutionary Computation*, vol. 17, no. 2, pp. 135 – 166, 2009.

[38] R. Purshouse and P. Fleming, "On the evolutionary optimization of many conflicting objectives," *Evolutionary Computation, IEEE Transactions on*, vol. 11, no. 6, pp. 770 – 784, dec. 2007.

[39] D. W. Corne and J. D. Knowles, "Techniques for highly multiobjective optimisation: some nondominated points are better than others," in *Proceedings of the 9th annual conference on Genetic and evolutionary computation*, ser. GECCO '07. New York, NY, USA: ACM, 2007, pp. 773 – 780.

[40] H. Ishibuchi, N. Tsukamoto, and Y. Nojima, "Evolutionary many-objective optimization: A short review," in *Evolutionary Computation, 2008. CEC 2008. (IEEE World Congress on Computational Intelligence). IEEE Congress on*, june 2008, pp. 2419 –2426.

[41] M. Ortega and F. Rubio, "Systematic design of weighting matrices for the h_∞ mixed sensitivity problem," *Journal of Process Control*, no. 14, pp. 89 – 98, 2004.

[42] C. A. C. Coello, "Evolutionary algorithms in control systems engineering: a survey," *Theorical and numerical constraint-handling techniques used with evolutionary algorithms: a survey of the state of the art*, no. 191, pp. 1245 – 1287, 2002.

[43] E. Mezura-Montes and C. A. C. Coello, "Constraint-handling in nature-inspired numerical optimization: Past, present and future," *Swarm and Evolutionary Computation*, no. 0, pp. –, 2011.

[44] K. Deb, "An efficient constraint handling method for genetic algorithms," *Computer Methods in Applied Mechanics and Engineering*, vol. 186, no. 2-4, pp. 311 – 338, 2000.

[45] P. Bonissone, R. Subbu, and J. Lizzi, "Multicriteria decision making (mcdm): a framework for research and applications," *Computational Intelligence Magazine, IEEE*, vol. 4, no. 3, pp. 48 –61, aug. 2009.

[46] J. B. Kollat and P. Reed, "A framework for visually interactive decision-making and design using evolutionary multi-objective optimization (video)," *Environmental Modelling & Software*, vol. 22, no. 12, pp. 1691 – 1704, 2007.

[47] A. Inselberg, "The plane with parallel coordinates," *The Visual Computer*, vol. 1, pp. 69–91, 1985, 10.1007/BF01898350.

[48] X. Blasco, J. Herrero, J. Sanchis, and M. Martínez, "A new graphical visualization of n-dimensional pareto front for decision-making in multiobjective optimization," *Information Sciences*, vol. 178, no. 20, pp. 3908 – 3924, 2008.

[49] G. Reynoso-Meza, X. Blasco, and J. Sanchis, "Diseño multiobjetivo de controladores pid para el benchmark de control 2008-2009," *Revista Iberoamericana de Automática e Informática Industrial*, vol. 6, no. 4, pp. 93 – 103, 2009.

[50] E. Zio and R. Razzo, "Multiobjective optimization of the inspection intervals of a nuclear safety system: A clustering-based framework for reducing the pareto front," *Annals of Nuclear Energy*, no. 37, pp. 798–812, 2010.

[51] E. Zio and R. Bazzo, "Level diagrams analysis of pareto front for multiobjective system redundancy allocation," *Reliability Engineering & System Safety*, vol. 96, no. 5, pp. 569 – 580, 2011.

[52] H. Safikhani, M. Akhavan-Behabadi, N. Nariman-Zadeh, and M. M. Abadi, "Modeling and multi-objective optimization of square cyclones using cfd and neural networks," *Chemical Engineering Research and Design*, vol. 89, no. 3, pp. 301 – 309, 2011.

[53] C. A. Mattson and A. Messac, "Pareto frontier based concept selection under uncertainty, with visualization," *Optimization and Engineering*, vol. 6, pp. 85 – 115, 2005, 10.1023/B:OPTE.0000048538.35456.45.

[54] P. Wen and T.-W. Lu, “Decoupling control of a twin rotor mimo system using robust deadbeat control technique,” *Control Theory Applications, IET*, vol. 2, no. 11, pp. 999 – 1007, nov. 2008.

[55] J.-G. Juang, R.-W. Lin, and W.-K. Liu, “Comparison of classical control and intelligent control for a mimo system,” *Applied Mathematics and Computation*, vol. 205, no. 2, pp. 778 – 791, 2008, special Issue on Advanced Intelligent Computing Theory and Methodology in Applied Mathematics and Computation.

[56] S. Montes de Oca, V. Puig, M. Witczak, and J. Quevedo, “Fault-tolerant control of a two-degree of freedom helicopter using lpv techniques,” jun. 2008, pp. 1204 –1209.

[57] C. Gabriel, “Modelling, simulation and control of a twin rotor mimo-system.” Master’s thesis, Universitat Politècnica de València., Avalaible at http://personales.upv.es/gilreyme/mood4ct/files/TRMS.zip, 2009.

[58] K. J. Åström, *Control system design*, 2002.

[59] M. Ge, M.-S. Chiu, and Q.-G. Wang, “Robust pid controller design via lmi approach,” *Journal of process control*, no. 12, pp. 3 – 13, 2002.

[60] R. Toscano, “A simple robust pi/pid controller design via numerical optimization approach,” *Journal of process control*, no. 15, pp. 81 – 88, 2005.

[61] E. N. Goncalves, R. M. Palhares, and R. H. Takahashi, “A novel approach for h_2/h_∞ robust pid synthesis for uncertain systems,” *Journal of process control*, no. 18, pp. 19 – 26, 2008.

[62] K. Astrom, H. Panagopoulos, and T. Hagglund, “Design of pi controllers based on non-convex optimization,” *Automatica*, vol. 34, no. 5, pp. 585 – 601, 1998.

[63] H. Panagopoulos, K. Astrom, and T. Hagglund, “Design of pid controllers based on constrained optimisation,” *Control Theory and Applications, IEE Proceedings -*, vol. 149, no. 1, pp. 32 – 40, jan. 2002.

[64] K. J. Astrom and L. Rundqwist, “Integrator windup and how to avoid it,” in *American Control Conference*, 1989, pp. 1693 – 1698.